Title

Kinetic Analysis of In Vitro Pre-mRNA Splicing in HeLa Nuclear Extract

Authors

Mueller, William F

Hertel, Klemens J

Publication Date

2014

DOI

10.1007/978-1-62703-980-2_12

Chapter 12

Kinetic Analysis of In Vitro Pre-mRNA Splicing in HeLa Nuclear Extract

William F. Mueller and Klemens J. Hertel

Abstract

Kinetic analysis of in vitro splicing is a valuable technique for understanding splicing regulation. It allows the determination of specific contributions from functional elements for the efficient removal of introns. This chapter will describe the rationale and approach employed to use kinetic analysis to evaluate an in vitro splicing reaction using radiolabeled pre-mRNA incubated in splicing-competent HeLa nuclear extract (NE).

Key words Splicing, Kinetics, In vitro splicing, Splicing rates, Alternative splicing

1 Introduction

In vitro splicing assays have been used to reliably discover new aspects of alternative splicing for many years [1–10]. The ability to manipulate the biochemical system where splicing reactions take place has illuminated the steps of the reaction, the molecular machinery required, and their regulation as splicing occurs. Although cell transfection and subsequent analysis are closer physiologically to a regulated splicing event, they lack the experimental flexibility of the in vitro system. That flexibility allows the study of specific RNA elements, trans-acting factors, and their unique effects that are otherwise difficult to determine in vivo or in cell culture.

There are differences between in vitro and cell culture splicing experiments. The rate of splicing in vitro is much slower than that which occurs in a cell [7, 11]. In vitro splicing occurs without nuclear compartmentalization, allowing the splicing machinery to be decoupled from the transcriptional machinery. While this permits characterization of specific sequence elements influence on splicing, it probably contributes to the decrease in the splicing rate in vitro as spliceosomal recruitment occurs co-transcriptionally in cells [12, 13]. Despite this drawback, the study of *cis*- and *trans-acting* splicing regulatory elements has shown that their actions in cell transfection and in vitro experiments yield parallel outcomes [4, 14].

Klemens J. Hertel (ed.), *Spliceosomal Pre-mRNA Splicing: Methods and Protocols*, Methods in Molecular Biology, vol. 1126, DOI 10.1007/978-1-62703-980-2_12,

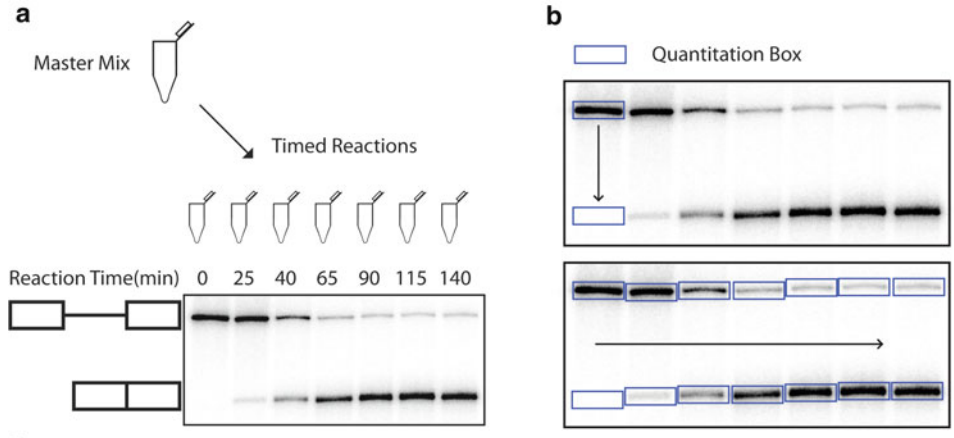

c

Time (min):	0	25	40	65	90	115	140	
Unspliced Signal	16127.936	12894.287	5235.818	2206.783	1510.565	1203.106	1453.320	>Data from Experiment
Spliced Signal	27.529	966.624	3716.618	7995.980	11042.765	13187.691	12497.682	
Total Signal	16155.466	13860.911	8952.436	10202.763	12553.330	14390.797	13951.003	>Calculated Data
Fraction Spliced	0.002	0.070	0.415	0.784	0.880	0.916	0.896	

Fig. 1 Analysis and quantitation of the gel scan. (**a**) The timed reactions run out on the gel allow observation of splicing over time. This is observed as the shift in band intensity from the higher pre-mRNA band to the lower spliced RNA band. Cartoon at left depicts the spliced and unspliced RNAs. (**b**) Quantitation boxes should be put around the bands as depicted. (**c**) The values (adjusted for background) for each time point/lane are found in the table. Total signal is the addition of the spliced and unspliced values. Fraction spliced is calculated per time point as the spliced value divided by the total signal. This is then plotted against time and fit with the rate equation to determine a rate constant

The kinetic analysis of in vitro splicing takes advantage of the small amount of pre-mRNA substrate required and the excess of splicing factors contained within the nuclear extract. This allows easy calculation of a rate constant using a pseudo-first-order rate approximation. When following along the time course of a splicing reaction, the first appearance of spliced product can be delayed [7]. This product appearance lag seems to be dependent on the efficiency of intron removal. Reactions that are less efficient or substrates that contain weaker splicing signals typically display longer lags. Once the reaction has proceeded past the lag phase, it enters the linear phase in which it exhibits reliable product appearance until the endpoint of the reaction is reached. That appearance of product can be measured and then fit to the first-order reaction model for the formation of spliced product: $A = C \times (1 - e^{-kt})$ where A is the fraction spliced, C is the fraction spliced at the endpoint of the reaction, k is the apparent rate constant, and t is time from the end of the lag period (*see* Figs. 1 and 2). This equation is a derivative of the standard reactant decay description $A = A_o \times e^{-kt}$. This rate equation describes an ideal reaction scenario where product formation initiates immediately and reaches 100 % completion. In practice, this is generally not the case so some fraction of the

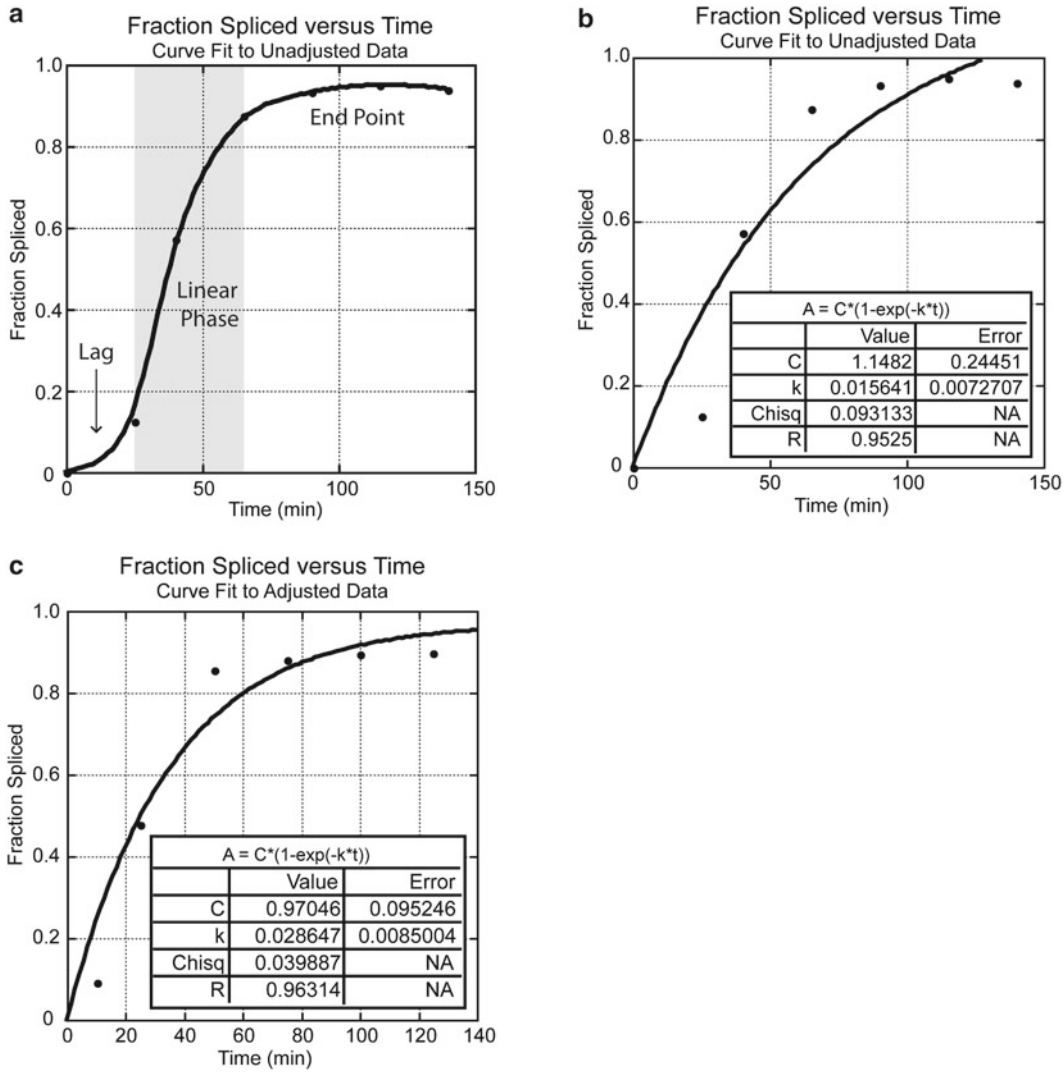

Fig. 2 Plotting and analysis of splicing data. (**a**) The data from Fig. 1c was plotted and fit with a smooth curve to depict the phases of the reaction. There is a slight lag, followed by the linear phase, followed by the endpoint phase. Due to the lack of change between the last three time points, we determine that the endpoint has been reached. (**b**) The data is then fit with a curve following the first-order rate equation. The equation is meant for an ideal reaction and thus gives a final value for *C* that is greater than 1. (**c**) Plotted values after adjusting for time. With the time adjustment, the calculated value for *C* is less than 1 suggesting this value is more accurate. This brings the splicing rate for this reaction to 0.029/min

pre-mRNA supplied may never be used as a splicing substrate. Fluctuations in lag time and overall fractions spliced will differ between NE preparations and pre-mRNA substrates.

The difference in kinetics between experimental treatments of splicing reactions has allowed the discovery of multiple regulatory mechanisms. Here, we describe the approach to carry out a basic

kinetic analysis of an in vitro splicing reaction. However, this protocol can be altered to determine other aspects of intron removal. For example, through the addition or depletion of regulatory proteins, one can determine during which step of splicing a specific action is taking place or when a specific factor influences the outcome of splice site recognition [14–17]. Furthermore, slight alterations in the gel type and reaction processing allow the visualization of different spliceosomal complexes and, thus, an analysis of their assembly kinetics [6, 14]. Biochemical tricks can be used to stall spliceosomal assembly at various stages thereby permitting further insights into the kinetics of splicing [6, 18, 19].

2 Materials

The in vitro splicing reaction is described in detail in Chapter 11. To obtain sufficient data point to carry out a kinetic analysis, multiple splicing reactions of identical composition need to be set up. They will be the same as are required to test kinetics of the in vitro splicing reaction.

1. Reagents as in Chapter 11, but sufficient amounts for multiple reactions.
2. Imaging system to quantitate signal from the labeled RNA off of the gel (such as Bio-Rad PhosphorImager).
3. Computer with suitable analysis and graphing software that allows line fitting to an input equation (such as Bio-Rad Quantity One in combination with KaleidaGraph™).

3 Methods

Carry out all steps of the reaction on ice unless otherwise stated.

1. Thaw reagents as in in vitro splicing reaction (Chapter 11).
2. Determine time points needed and the Master Mix (MM) reaction volume: (# of time points + 1) × volume per reaction = MM volume (*see* **Note 1**).
3. Mix reagents as in Chapter 11.
4. Reactions should be aliquoted into separate tubes of equal volume and kept on wet ice. This means that there will be one MM tube and one tube for each time point chosen, for example, if the time course is for 2+h with 7 time points, the MM tube will be divided into tubes to be incubated for 0, 25, 40, 65, 90, 115, and 140 min. Place the time 0 tube on dry ice immediately after mixing the reaction to prevent the reaction from progressing.

5. Incubate reactions at 30 °C for the desired length of time for each time point. Most in vitro splicing reactions should reach completion within ~2 h.
6. Once reactions have reached their time point, place on dry ice to stop the reaction from progressing, i.e., after 25 min, the 25 min time point tube should be removed from the water bath and placed on dry ice. To freeze the tube and stop the reaction quickly, crush the dry ice into powder so the tube can be immersed.
7. Once the reactions have finished, prepare the samples, and load and run them on the gel as in Chapter 11.
8. Expose the gel to film or preferably a PhosphorImager screen or similar equipment for 1 h to overnight, depending on the radioactivity of the pre-mRNA used (*see* Chapter 11).
9. Once the screen has been exposed, scan the screen for quantitation and subsequent use in the analysis software. The appearance of spliced product on the scan can be observed by a decrease over time in the full length unspliced pre-mRNA and an accompanying increase over time in the correctly sized product band (*see* Fig. 1a).
10. Determine the level of signal for the bands in each lane on the scan pertaining to fully spliced products and the unspliced pre-mRNA. This should be done using suitable quantification software compatible with your imaging system (such as Bio-Rad Quantity One). Using the box quantification tool, a small box containing the largest band should be drawn. A copy of this box should be made and then used to quantify all other desired bands (*see* Fig. 1b and **Note 2**). The signal levels can then be used to calculate the total spliced signal in each lane. Do this by adding all the values determined for each lane/time point together, spliced products, as well as the unspliced band.
11. Determine the fraction spliced for each time point. The fraction spliced is the signal from the spliced product (or products) divided by the total amount of signal within a lane. This value should increase in an efficient splicing reaction as time progresses such that in the final time points there is very little change in the last values (signifying the endpoint has been reached). There is no loading control so comparison between lanes is not useful. Computing this value allows one to observe the changes in splicing that occur without trying to compare between lanes.

    Fraction spliced = Signal from spliced products/total signal from **step 10** (*see* Fig. 1c).
12. The fraction of spliced product and time data should be plotted as the time (*x*-axis) vs. fraction spliced (*y*-axis) for each time point taken. This plot should have at least two parts: a linear

increase to a point (linear phase) that then levels to a plateau or asymptote (endpoint phase; *see* Fig. 2a). Reaching the endpoint of the reaction is important for the proper determination of the rate constant (*see* **Note 3**). There may also be a lag before the linear phase of splicing occurs (*see* **Note 4**). This is due to the competition in the NE for the pre-mRNA by multiple groups of proteins that may impede splicing complex formation.

13. Determine the observed rate of splicing by fitting the data points to an equation that describes first-order rate kinetics (*see* Fig. 2b). This is appropriate because the splicing reaction contains an excess of splicing components and a limiting amount of pre-mRNA (*see* **Note 5**). Using appropriate graphing software, the reaction profile can be fit to the equation $A = C \times (1 - e^{-kt})$, where A is the fraction spliced, C is the fraction spliced at the endpoint of the reaction, k is the apparent rate constant, and t is the time.
14. Make any adjustments to the data to more accurately identify the splicing portion of the reaction. A lag in the splicing of the pre-mRNA can be observed by a period of very little appearance of spliced product for the first ~25 min of the splicing reaction. If there is a lag at the beginning of the in vitro splicing reaction, it may be helpful to adjust the time course by subtracting the length of the lag time from each time point taken. To account for the delay in timing, subtract the amount of time before splicing is observed from all time values. To do this, draw a line along the slope of the linear phase of the splicing reaction—in Fig. 2 the 25–65 min time points. Then use the x-intercept of that line as the lag time and subtract it from each time point. The adjusted profile will more closely follow the actual kinetics of splicing as opposed to including the kinetics of the proteins initial competition for the pre-mRNA (*see* Fig. 2c). Additionally, the fit curve may run to a maximum spliced fraction that is greater than 1. If this is the case, it is most likely due to a need for more time points to more accurately follow the reaction or for a longer reaction time to better determine the endpoint of the reaction (*see* **Notes 3** and **4**).
15. Replot the adjusted data and redetermine the curve fit. Rate constants of different pre-mRNAs or different reaction conditions can then be compared to determine the influence of splicing effectors. Not adjusting the data may result in inaccurate results for values computer using the first-order rate equation. This is usually due to insufficient time points (not accurately following the changes over time or not reaching the endpoint of the reaction) or not accounting for the lag period when splicing is not yet occurring.

4 Notes

1. The number of time points required depends on the resolution required for the rate constant. More data points assure a more accurate rate determination. An initial time course can be run with evenly spaced time points (every 10–15 min.) that will allow to determine the general shape of the reaction analyzed. Following this first attempt, taking more time points during the portions of the reaction in the linear phase and its slow transition into the end phase are recommended. More data in the linear phase is important because this is the area where the most striking changes are observed. More data toward the endpoint is necessary to accurately define maximal splicing levels.
2. Identical volume quantitation areas ensure differences between bands are not due to quantification box volume. A box does not have to be used; other shapes are usable as long as they are all the same around each band. Additionally, make sure to account for background signal either with a setting within the quantification program or by making an extra quantification box around an area where there is no band, giving a value that can then be subtracted from all other bands, removing the background signal. Additionally, make sure the boxes do not overlap.
3. The maximum product formation or fraction of spliced product at the endpoint of the reaction will be different for every pre-mRNA evaluated. Less efficient nuclear extracts and pre-mRNAs with poorer splice sites may have a lower fraction of spliced product at the endpoint of the reaction. This should be verified experimentally by carrying out splicing reactions with extended time points (past 2 h). By carrying out longer experiments, the true endpoint of the reaction can be determined eliminating any error that may occur due to the estimations of the software and curve fitting functions.
4. Determination of the reaction lag time adjustment allows a better fit for the rate equation to the splicing phase of the reaction. Pre-mRNAs that have less binding potential with splicing components have been noted to have longer lag times, suggesting that the lag is occurring due to competition for binding along the pre-mRNA molecule. After this lag, the reaction follows a pseudo-first-order reaction rate profile. This is what is modeled by the rate equation used, the initial linear appearance of product followed by a hyperbolic approach to an asymptotic maximum of product formation.
5. Even though the reaction is second order, based on the concentrations of NE and the pre-mRNA, it can be analyzed as a first-order reaction because the [NE] is in such excess over the [pre-mRNA] that the [NE] does not change over the course of the reaction, i.e., pseudo-first-order reaction conditions

(~2 μg/μL of protein vs. 0.01–0.1 nM RNA in the reaction). This does mean that if you are adding splicing components to the reaction, they should be added to saturating amounts so as to make sure they interact with all radiolabeled pre-mRNAs in the reaction.

Acknowledgement

Research in the Hertel laboratory is supported by NIH (RO1 GM62287 and R21 CA149548).

References

1. Black DL, Chabot B, Steitz JA (1985) U2 as well as U1 small nuclear ribonucleoproteins are involved in premessenger RNA splicing. Cell 42(3):737–750
2. Tarn WY, Steitz JA (1994) SR proteins can compensate for the loss of U1 snRNP functions in vitro. Genes Dev 8(22):2704–2717
3. Tarn WY, Steitz JA (1995) Modulation of 5′ splice site choice in pre-messenger RNA by two distinct steps. Proc Natl Acad Sci USA 92(7):2504–2508
4. Krainer AR, Maniatis T, Ruskin B et al (1984) Normal and mutant human beta-globin pre-mRNAs are faithfully and efficiently spliced in vitro. Cell 36(4):993–1005
5. Ruskin B, Krainer AR, Maniatis T et al (1984) Excision of an intact intron as a novel lariat structure during pre-mRNA splicing in vitro. Cell 38(1):317–331
6. Kotlajich MV, Crabb TL, Hertel KJ (2009) Spliceosome assembly pathways for different types of alternative splicing converge during commitment to splice site pairing in the A complex. Mol Cell Biol 29(4):1072–1082. doi:10.1128/MCB.01071-08, MCB.01071-08 [pii]
7. Hicks MJ, Lam BJ, Hertel KJ (2005) Analyzing mechanisms of alternative pre-mRNA splicing using in vitro splicing assays. Methods 37(4):306–313
8. Zhou Z, Sim J, Griffith J, Reed R (2002) Purification and electron microscopic visualization of functional human spliceosomes. Proc Natl Acad Sci USA 99(19):12203–12207
9. Deckert J, Hartmuth K, Boehringer D et al (2006) Protein composition and electron microscopy structure of affinity-purified human spliceosomal B complexes isolated under physiological conditions. Mol Cell Biol 26(14):5528–5543. doi:10.1128/MCB.00582-06, 26/14/5528 [pii]
10. Hicks MJ, Mueller WF, Shepard PJ et al (2010) Competing upstream 5′ splice sites enhance the rate of proximal splicing. Mol Cell Biol 30(8):1878–1886. doi:10.1128/MCB.01071-09, MCB.01071-09 [pii]
11. Audibert A, Weil D, Dautry F (2002) In vivo kinetics of mRNA splicing and transport in mammalian cells. Mol Cell Biol 22(19):6706–6718
12. Kornblihtt AR, de la Mata M, Fededa JP et al (2004) Multiple links between transcription and splicing. RNA 10(10):1489–1498
13. Hicks MJ, Yang CR, Kotlajich MV et al (2006) Linking splicing to Pol II transcription stabilizes pre-mRNAs and influences splicing patterns. PLoS Biol 4(6):e147
14. Erkelenz S, Mueller WF, Evans MS et al (2013) Position-dependent splicing activation and repression by SR and hnRNP proteins rely on common mechanisms. RNA 19(1):96–102. doi:10.1261/rna.037044.112
15. Lam BJ, Bakshi A, Ekinci FY et al (2003) Enhancer-dependent 5′-splice site control of fruitless pre-mRNA splicing. J Biol Chem 278(25):22740–22747. doi:10.1074/jbc.M301036200, M301036200 [pii]
16. Lam BJ, Hertel KJ (2002) A general role for splicing enhancers in exon definition. RNA 8(10):1233–1241
17. Hertel KJ, Maniatis T (1999) Serine-arginine (SR)-rich splicing factors have an exon-independent function in pre-mRNA splicing. Proc Natl Acad Sci USA 96(6):2651–2655
18. Fox-Walsh KL, Dou Y, Lam BJ et al (2005) The architecture of pre-mRNAs affects mechanisms of splice-site pairing. Proc Natl Acad Sci USA 102(45):16176–16181
19. Lim SR, Hertel KJ (2004) Commitment to splice site pairing coincides with A complex formation. Mol Cell 15(3):477–483